Modeling on runoff concentration caused by rainfall on hillslopes and application in Maoping slope*

LIU Qingquan** and LI Jiachun

(Institute of Mechanics, Chinese Academy of Sciences, Beijing 100080, China)

Received January 9, 2006; revised January 16, 2006

Abstract Based on the fact that the concentration flowlines of overland flow depend on the surface landform of hillslope, a kinematic wave model was developed for simulating runoff generation and flow concentration caused by rainfall on hillslopes. The model-simulated results agree well with the experimental observations. Applying the model to the practical case of Maoping slope, we obtained the characteristics of runoff generation and infiltration on the slope. Especially, the simulated results adequately reflected the confluent pattern of surface runoff, which offers a scientific foundation for designing the drainage engineering on the Maoping slope.

Keywords: complex hillslope, rainfall, infiltration, overland flow, runoff concentration, Maoping slope.

Rainfall infiltration is a significant factor that affects the stability of slopes. Commonly, a large amount of rainwater infiltration can change the pore pressure field, stress field, medium strength and deadweight of slopes, which will badly affect the stability of landslides due to the increases of the pore pressure and the volume weight of slopes and the rapid decreases of the suction and shear strength of soil[1—5]. Obviously, rainfall plays an important role in the process of slope failure, and so the effective drainage is one of the important engineering measures for the protection of landslides.

For a slope, especially a large slope, variation methods are commonly applied for slope's synthesis administration. The drainage engineering is often one of the most significant engineering measures. The drainage methods often used in engineering include the periphery intercepting ditch, interior drain, drainage blind ditch, drainage bore, drainage gallery, grouting preventing water, and etc. Among them, the surface drainage is one of the most effective engineering measures. However, understanding the internal process of runoff generation on slope surface is the key to properly design the surface drainage engineering. In practical cases, the surface landform of slopes is very complex, and the overland flow caused by rainfall is also very complex because of the effect of irregular topography. Therefore, delicately simulating the concentrated flow routing of overland flow on slopes is of primary importance for drainage engineering design.

Theoretically, two-dimensional (2-D) equation of water flow is a good selection to describe the directions of overland flow. However, the overland flow caused by rainfall is a kind of special flow different from the general stream flows for its very small water depth, complex boundaries and visible up-and-down landform, which greatly affect the flow characteristics of overland flow. Therefore, it is not easy to apply 2-D shallow water equations to overland flow. Till now, the research results in this aspect are rather limited. Scoging[6] firstly studied the process of runoff converging on hillslopes, and developed a distributed model of overland flow. The model employed two-dimensional cells (or grid elements) and one-dimensional kinematic wave model to simulate overland flow in every cell. The pattern of concentrated flow approximate to the real pattern was obtained using this model. However, this model assumed that all the water of each element flows out only from a lower side, which is not true, and thus leading to a limitation that may be incorrect under some situations. In addition, the flow directions must be artificially determined firstly before calculation according to the landform of slopes, which resulted in the inconvenient application of the model. Subsequently, Govin-

* Supported by National Natural Science Foundation of China (Grant No. 10332050), the Major State Basic Research Development Program of China (Grant No. 2002CB412703), and the Knowledge Innovation Project of Chinese Academy of Sciences (Grant No. KJCX2-SW-L1-4)

** To whom correspondence should be addressed. E-mail: qqliu@imech.ac.cn

daraju et al.[7] and Tayfur[8] also studied the simulation method of 2-D flow of overland flows by extending the kinematic wave theory from its 1-D form to 2-D form. However, in their models, the flow directions need to be artificially determined based on the surface topography of slopes. Michael and Refsgaard[9], Cao et al.[10] applied the distributed hydrologic models to simulate the converging process of runoff caused by rainfall in small catchments. Their models improved the determination of out flow where the water of each element can flow out from one side or one corner point of element, but the direction of flow still needs to be artificially determined firstly before calculation. In addition, these models adopted a simply total water amount balance to calculate the water flow in each element, which cannot effectively reflect the dynamic process of overland flows. On the basis of these investigations, by decomposing the water flow into two directions in a calculation element, we developed a 2-D model of overland flow that can reasonably simulate the process of overland flow concentration[11,12]. However, the method of determining the flow directions is rather complex, which leads to some limitations.

The objective of this study is to find a more efficient and accurate calculating method to establish a dynamics model to automatically and reasonably simulate the concentration process of overland flow on hillslopes. We apply the model to the practical case of Maoping slope, Qingjiang River to analyze the characteristics of runoff concentration caused by rainfall on Maoping slope in detail, so as to offer a scientific foundation for designing the surface drainage engineering in the protection of Maoping landslide.

1 Model of runoff concentration on slopes

Overland flow is closely related with the soil infiltration, and is the result of rainfall and soil infiltration interaction. Although not participating in the movement of overland flow, the soil infiltration process directly affects the process and amount of runoff yield. Inversely, the movement of overland flow also affects the soil infiltration in a certain degree. However, because the influence of overland flow on soil infiltration is rather weak, commonly, overland flow and infiltration have been extensively studied as separate components[13]. The conventional approach has been through the rainfall-excess concept[14].

Because of the different climates and surface conditions, the runoff generation caused by rainfall is divided into two types: infiltration excess (Horton) runoff and saturation excess (Dunne) runoff. Saturation excess runoff generally occurs in the drainage basin with high groundwater level. Rainfall infiltration could make the moisture of soil quickly reach saturation, and the part of runoff infiltrates at a steady rate of soil permeation form subsurface runoff. Inversely, infiltration excess runoff does not form groundwater runoff. Only when rainfall intensity excesses the infiltration rate of soil, runoff occurs on the surface of slopes. The main difference is whether or not to form the groundwater runoff. In the situation of saturation runoff, the part of rainfall will flow in the form of groundwater, and for infiltration excess runoff, the whole infiltration water will store in the unsaturated zone of soil to turn into the loss quantity of rainfall instead of groundwater runoff. In the present study, the concentration process of surface runoff rather than infiltration process of rainfall was concerned. In addition, Maoping slope is a small slope with low groundwater level. This study will aim at the influence of a rainstorm on runoff generation of slope. Consequently, applying infiltration excess runoff model is rather appropriate to simulate the surface runoff generation on the Maoping slope.

1.1 Infiltration formula

Soil infiltration is a precursory process for runoff formation. Generally, its influencing factors include the saturate conductivity (or infiltration coefficient) of soil, initial water content, saturate volumetric water content, cumulative infiltration quantity, soil properties, and etc. At the beginning stage, the rainfall intensity is commonly greater than the soil infiltrating capability, the real infiltration rate of soil is equal to the rainfall intensity. With the time progress of infiltration, the infiltration capacity reduces gradually and finally reaches an appropriately constant value. Based on this knowledge, the famous Green-Ampt model with explicit physical meaning was selected to describe the soil infiltration process, which may be written as

$$i = \frac{\mathrm{d}I}{\mathrm{d}t} = K[1 + (\theta_s - \theta_i)S/I],$$

$$I = Kt + S(\theta_s - \theta_i)\ln\left(1 + \frac{I}{S(\theta_s - \theta_i)}\right), \quad (1)$$

where i is the infiltration rate (m/s), I is the cumulative infiltration quantity (m), K is the saturated hydraulic conductivity of soil (or infiltration coeffi-

cient) (m/s), θ_s is the saturated volumetric water content, i.e. the effective porosity (cm^3/cm^3), θ_i is the initial volumetric water content (cm^3/cm^3), and S is the soil suction (m).

The Green-Ampt equation is applied to ponding water infiltration on dry soils. However, there is no ponding water at the beginning stage of rainfall in practical situations. Mein and Larson[15] generalized it to infiltration during rainfall. Suppose p is the steady rainfall intensity, when i equals p, the ponding occurs according to the Hortonian mechanism. The cumulative infiltration at the time, I_p, can be derived as follows:

$$I_p = \frac{(\theta_s - \theta_i)S}{(p/K) - 1}, \tag{2}$$

from which the ponding time is obtained as

$$t_p = I_p/p. \tag{3}$$

Thus, the infiltration rate in the whole overland flow process can be expressed as

$$\begin{aligned} i &= p, && t \leqslant t_p \\ i &= K[1 + (\theta_s - \theta_i)S/I], && t > t_p \end{aligned} \tag{4}$$

In order to express infiltration as a function of time, one has

$$K(t - t_p) = I - I_p - S(\theta_s - \theta_i)\ln\left(\frac{I + S(\theta_s - \theta_i)}{I_p + S(\theta_s - \theta_i)}\right), \quad t > t_p. \tag{5}$$

By the above formulas, the real infiltration process can be simulated reasonably.

1.2 Kinematic wave equation for overland flow

Because of the very thin depth of overland flow and the complicated boundary conditions, it is a tough task to describe the movement of this kind of flow appropriately. As for surface runoff, most researchers prefer to describe it by the so-called kinematic wave theory. Actually, it is a simplified form of the 1-D St. Venant model. The main assumption of the kinematic wave model is that the gravity component along the slope is equal to the resistance force ($S_f = S_0 = \sin\theta$), and thus a concise relationship between discharge and water depth is established by borrowing the Chezy's resistant formula. The investigation by Woolhiser and Liggett[16] validated that when the kinematic wave number $K > 10$ (In practice, the kinematic wave number is certainly much greater than 10 in most situations), the kinematic wave model can describe overland flow quite well. Therefore, kinematic wave approach is widely accepted for modeling overland flow on hillslopes. For steep slopes, the kinematic wave equations can be written as[17,18]

$$\begin{aligned} &\frac{\partial h}{\partial t} + \frac{\partial q}{\partial x} = p\cos\theta - i, \\ &q = \frac{1}{n}h^{5/3}S_0^{1/2}, \end{aligned} \tag{6}$$

where x (m) is the distance down slope, h (m) is the water depth, q ($m^2 \cdot s^{-1}$) is the unit width discharge, θ is the inclination angle of slope (in degree), n ($s \cdot m^{-1/3}$) is the Manning roughness coefficient, and S_0 is the slope gradient ($S_0 = \sin\theta$).

The overland flow concentration on an irregular hillslope is a two-dimensional process and its simulation requires a two-dimensional flow model. Therefore, it was considered appropriate to extend the theory from its 1-D form to 2-D form. Based on the previous experience, the kinematic wave theory can be extended to its 2-D form[11,12]:

$$\begin{cases} \dfrac{\partial h}{\partial t} + \dfrac{\partial q_x}{\partial x} + \dfrac{\partial q_y}{\partial y} = p\cos\theta - i \\ q = uh = \dfrac{1}{n}h^{\frac{5}{3}}S_0^{\frac{1}{2}} \\ q_x = q\cos\gamma \\ q_y = q\sin\gamma \end{cases}, \tag{7}$$

where q is the unit width discharge of runoff in the flow direction; u is the runoff velocity in the flow direction, q_x and q_y are the unit width discharge components in the x and y directions, respectively; and γ is the angle between the flow direction and the x coordinate.

1.3 Determining and controls of flow directions

From Eq. (7), it is obvious that the expressions originate from the 1-D formulation of the kinematic wave theory. Then, the runoff discharge (or flow velocity) can be divided into the x and y directions according to the flow direction. Thus, one feasible wayout is to introduce 2-D grids on the slope surface. The flow in a calculation cell (or grid element) is simulated by the one-dimensional kinematic wave model at first, and then cells were connected to each other by distinguishing the flow direction in every cell, and the flow discharge was divided into x and y directions according to the geometry of the topography of every cell. Finally, runoff was computed for whole hillslope. Therefore, determining and control of the flow directions is one key step in the model.

In the previous models, the flow direction must be artificially determined firstly according to the landform of slopes[6—10], and all the water of each element was assumed to flow out only from a lower side, which is not true, and may result in the inconvenient application of the model. Based on the fact that the flow direction depends on the landform of hillslopes, in the present model, the water of every cell may flow out from two sides of the cell and flow into two neighbouring cells. Therefore, we deal with the water in each cell to flow to two lower adjacent grids, and divide the flow discharge into the x and y directions in each cell.

As shown in Fig. 1, the hillslope surface is partitioned into rectangular grids or cells. A rectangular grid is the projection of the grid onto the horizontal plane. In fact, the four points of an element in the practical space are not in the same plane. Assuming the element plane to be a bilinear element, one can express:

$$z = (ax + b)(cy + d), \tag{8}$$

where z is the height of the element; and x and y are the abscissa and ordinate, respectively. From Eq. (8), the relation between z and y is always linear for a fixed x, and the relation between z and x is always linear for a fixed y.

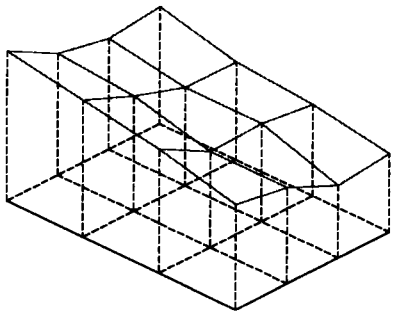

Fig. 1. Sketch of 2-D grids.

According to the bilinear element approach of calculation cell and employing coordinate transformation method, we have ever established a method to divide runoff into two directions[11,12]. Through transforming the projection area of the element to the fixed area $[-1,1]\times[-1,1]$, we may derive the equation of cell plane, further to obtain the obliquity of the center point of cell to represent the cell slope and the direction angle of flowline in the cell. This method is complex in practical application. Therefore, this study will employ a more simple method to divide the flow direction in a cell. That is, using the average slope to express the angle of calculation element, and applying the average slopes in the x and y directions to divide runoff into two directions.

As for a calculated element $ABCD$ shown in Fig. 2(a), assuming that the heights of four corner points are z_A, z_B, z_C, z_D, respectively; the dx and dy values are the projections on the horizontal plane of the grid step lengths in the x and y directions, respectively; and θ_x and θ_y are the average angles of grid in the x and y directions, respectively; we have approximately:

$$\tan\theta_x = \frac{1}{dx}\left[\frac{z_A + z_B}{2} - \frac{z_C + z_D}{2}\right] = \frac{1}{2dx}(z_A + z_B - z_C - z_D), \tag{9}$$

$$\tan\theta_y = \frac{1}{dy}\left[\frac{z_A + z_C}{2} - \frac{z_B + z_D}{2}\right] = \frac{1}{2dy}(z_A + z_C - z_B - z_D). \tag{10}$$

Consequently, the slope gradient of the element, i.e. the representative slope gradient θ, can be obtained as:

$$\tan\theta = \sqrt{\tan^2\theta_x + \tan^2\theta_y}, \tag{11}$$

i.e.

$$\theta = \arctan\sqrt{\tan^2\theta_x + \tan^2\theta_y}, \tag{12}$$

and the flow vector direction angle γ as shown in Fig. 2(b) can be expressed as:

$$\tan\gamma = \frac{\tan\theta_y}{\tan\theta_x} = \frac{dx}{dy}\left[\frac{z_A + z_C - z_B - z_D}{z_A + z_B - z_C - z_D}\right]. \tag{13}$$

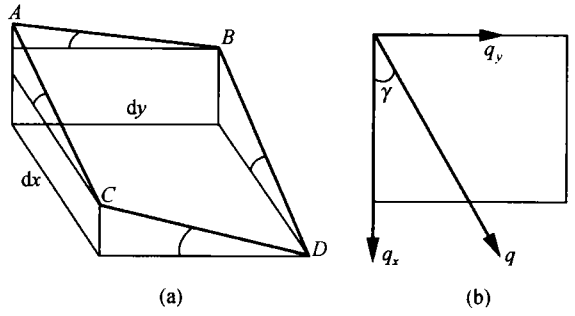

Fig. 2. Element flowline analysis. (a) Sketch of element dimension; (b) element flowline disintegration.

In this model, the water in every element is considered to flow out along the flow direction, and then flow into two adjacent grids. That is, the water in a cell is assumed to flow out from any point of a cell along the flow direction angle and flow into two neighbour cells. Thus, the water flowlines will intersect with two sides of grid. If the unit discharge is q, the

unit discharges in the x and y directions can be calculated, respectively, as

$$q_x = q\cos\gamma, \quad q_y = q\sin\gamma. \tag{14}$$

To express the average length of each element in space by Δx and Δy, we have

$$\Delta x = \mathrm{d}x/\cos(\theta_x), \quad \Delta y = \mathrm{d}y/\cos(\theta_y). \tag{15}$$

Consequently, the flow direction angle and the outflow discharge of each side in a calculated element can be calculated by the above formulas.

1.4 Discretization and solution of the equations

The flow continuum equation can be written as:

$$\frac{\partial h}{\partial t} + \frac{\partial F_x}{\partial x} + \frac{\partial F_y}{\partial y} = C, \tag{16}$$

where F_x and F_y express the unit discharge components in x and y directions, respectively; and C is the source item. Taking the calculation point at the center of a grid, the finite volume difference expression of Eq. (16) can be written as:

$$h_{i,j}^{n+1} = h_{i,j}^{n} - \frac{\Delta t}{\Delta\bar{x}\Delta\bar{y}}(F_{x_{i+\frac{1}{2},j}}\Delta Y_{i+\frac{1}{2},j} - F_{x_{i-\frac{1}{2},j}}\Delta Y_{i-\frac{1}{2},j} + F_{y_{i,j+\frac{1}{2}}}\Delta X_{i,j+\frac{1}{2}} - F_{y_{i,j-\frac{1}{2}}}\Delta X_{i,j+\frac{1}{2}}) + C_{i,j}^{n+1}\Delta t, \tag{17}$$

where Δt is the time step of calculation; $\Delta\bar{x}$ and $\Delta\bar{y}$ are the lengths of the calculation grid unit in x and y directions, respectively; and ΔX and ΔY with subscript are the real lengths of the cell in x and y directions, respectively.

Because every element does not have only an inflow cell and an outflow cell, applying the first-order backward difference operator, the inflow unit discharge is the total discharge of all inflow cells. In the same way, the outflow unit discharge represents the total discharge of all outflow cells.

2 Model validation

To verify the validity of the model, the process of runoff generation and flow concentration on a hillslope with an up-and-down landform were investigated experimentally at the National Key Laboratory of Soil Erosion and Dryland Farming in Loess Plateau in the Northwestern Institute of Water and Soil Conservation, Chinese Academy of Sciences. Rainfall was simulated by a drop-former type of artificial rainfall simulator, in which raindrops were formed at 16 m above the surface of test plot and the falling raindrops attained a fixed speed near the surface. The test plot was a 320 cm long, 100 cm wide, and 30 cm deep wooden-flume. The soil used in the experiment was the local loess of Yangling in the Shanxi Province of China. The soil was packed into the wooden flume with 30 cm deeps, and was controlled to reach a bulk density of 1.3 g/cm^3. The initial surface landform was an irregular surface that was artificially made before experiment. It is convenient to observe the process of runoff concentration caused by complex surface landform of slope. The slope gradient of the soil flume was secured at 10° during experiment. The rainfall intensity adopted in this experiment was 1.6 mm/min, and the rainfall duration was 1 hour. The process of runoff concentration was observed and the runoff volume was measured at the test plot outlet.

Due to the artificial irregular surface, at the beginning stage of experiment, runoff formed clear concentrated flow route, which demonstrates that the concentration of surface runoff depends on the landform of slopes. In experiment, the soil erosion caused by runoff results in a little evolvement of initial landform of the slope. However, these changes occur mainly in the groves of the slope, i.e. in the concentrated flow route, which mainly scoured the groves deep, and did not cause the change of runoff flow route. Therefore, the observed flowlines truthfully reflected the concentrated runoff route in the experiment.

Using the proposed model, the process of runoff generation and flow route concentration on the test plot were simulated. The model parameters used in simulation are selected as: the porosity of soil is 50.27%, the initial water content is 22.62%, the permeability coefficient of soil is 0.1 mm/min, the soil suction is 0.15 m, and the surface roughness coefficient is 0.03. The simulation results are shown in Figs. 3, 4.

Fig. 3 compares the observed and predicted runoff volumes and total discharges at the outlet of the test plot. Although the observed runoff data exhibits a little randomness, on the whole, the agreement between the observed and predicted results was good. And the simulated runoff volumes are in good agreement with the observed results. Fig. 4 (b) shows distributions of the simulated flow depths on the entire test plot at the runoff steady state. In Fig. 4(b), the position with the high values of the water depth is just the position where the water starts to converge on a route. Compared to the experimental results of Fig. 4 (a), the agreement between simula-

tion results and experimental observations is rather good. These comparisons show that the proposed model is capable of adequately simulating the processes of runoff generation and flowline concentration on hillslopes.

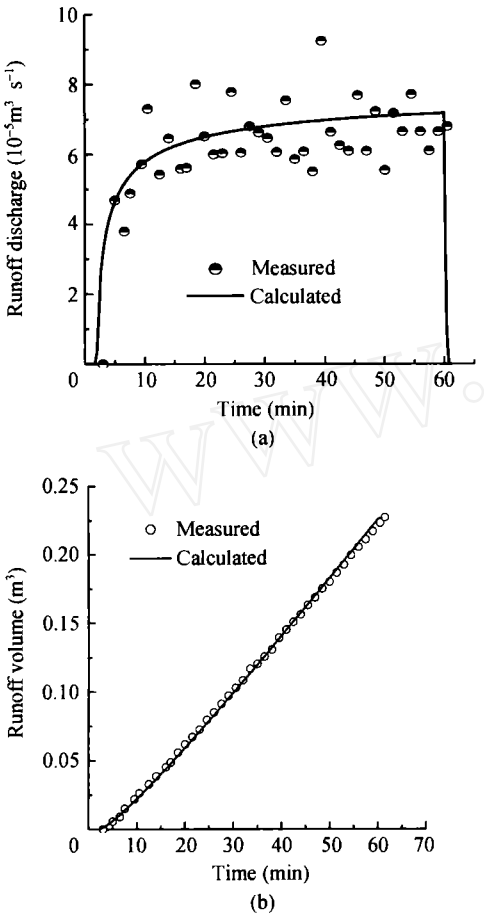

Fig. 3. Comparison of the observed and predicted runoff yield processes. (a) Runoff discharge; (b) runoff volume.

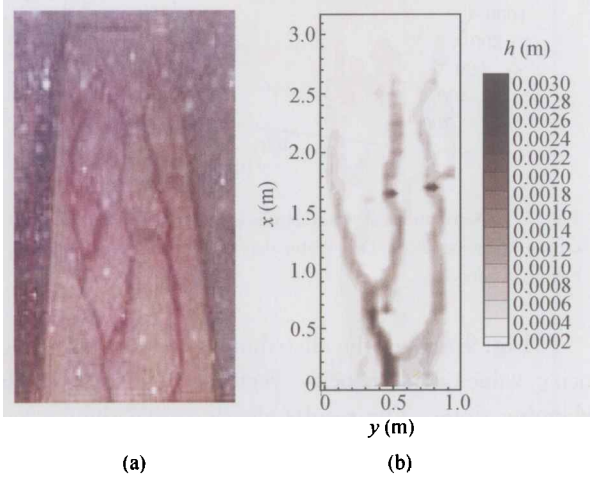

Fig. 4. Comparison of the observed and predicted concentrated flow route. (a) Flow visualization results of concentrated flow; (b) simulated results of runoff depth distribution.

3 Runoff yield and concentration on Maoping slope

3.1 Brief introduction of Maoping slope

The physical model is based on a practical slope, named Maoping slope, which is located on the left bank of Qingjiang River, Hubei, China. Maoping slope is one of the largest landslides in the Geheyan reservoir area, and with a distance of 6600 m from the dam. Since Geheyan reservoir began reserving water in 1993, the slope has drawn great attention due to its increasing deformation, which has reached 2100 mm according to the monitoring data. It is the potential of blocking up Qingjiang River once the slide occurs. Analysis shows that the reservoir reserving water and rainfall is the main reason of causing the revival of the landslide[19]. The whole slope likes a long and narrow stripe with a length of 1600 m, a width of 600 m and a total volume of 2350×10^4 m^3 as shown in Fig. 5. Its back edge is perched on 570 m above the sea level, the thickness of the sliding body is between 5 and 87 m with the average value of 40 m. The front edge part is rather steep with about 28—55 degrees, and other parts are relatively flat with about 15—20 degrees.

Fig. 5. Maoping slope, Qingjiang River.

3.2 Modeling area and model parameters

A regular rectangle region including the Maoping slope is selected as the simulated area. Selecting the longitudinal direction along the slope as the x coordinate, and transverse direction as the y coordinate, the calculation zone is shown in Fig. 6, where $0 \leqslant x \leqslant 1600$ m, $0 \leqslant y \leqslant 800$ m. The size of the grids is set as 20 m $\times$ 20 m and the number of grids is 80×40. To simplify the calculation, we assume that there is no inflow around boundaries, but there may be outflow around boundaries which completely depend on the landform condition and simulated results.

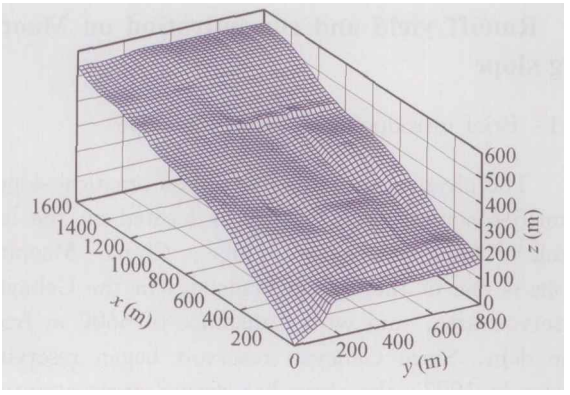

Fig. 6. Topography of simulated area.

The landform and vegetation conditions on the Maoping slope are complex, which may influence rainfall because of the trapping function of vegetation. In addition, the non-uniform distribution of vegetation covers on the Maoping slope can result in variation of soil porosity, initial water content, and soil permeability coefficient. However, due to the lack of practical observation, influences are not considered in the present model. For the study of the concentration process of surface runoff caused by a rainstorm, the vegetation cover condition will bring little effects on the concentration process and flow route of surface runoff. Consequently, using the present model is feasible to simulate the runoff concentration process on the Maoping slope. Although the distribution of soil parameters is non-uniform because of vegetation influence, we take the soil parameter as constant due to the very limited study area. According to the observation in the Maoping slope, the parameters of soil are selected as follows: the porosity of soil is 48%, the initial water content is 17%, the permeability coefficient of soil is 1.465×10^{-6} m/s, the soil suction is 0.2 m, and the surface roughness coefficient is 0.045.

3.3 Simulated results and analyses

3.3.1 Concentrated flow routing of runoff on slope surface

Taking the rainfall intensity of 60 mm/h, the process of runoff yield on Maoping slope is simulated by using the present model. The simulated results are shown in Figs. 7—9. Fig. 7 illustrates the distributions of the simulated runoff depths and unit discharges on the Maoping slope at 60 mins of rainfall. To clearly display the concentration flow route, Fig. 8 shows the plane distributions of the simulated runoff depths and unit discharges. In the figures, the position with deeper water depth is just the position of the concentrated flow route. The results show that there are two obvious concentrated flow routes on the Maoping slope. Compared with the real landform of the Maoping slope, the simulated results clearly reflect the influence of landform characteristics on surface runoff movement. Although there are no real observation results of surface runoff, there indeed are two obvious groves on the Maoping slope according to primary spot investigation. The simulated results demonstrate that the present model is able to perfectly simulate the runoff yield process on slopes with complex surface topography.

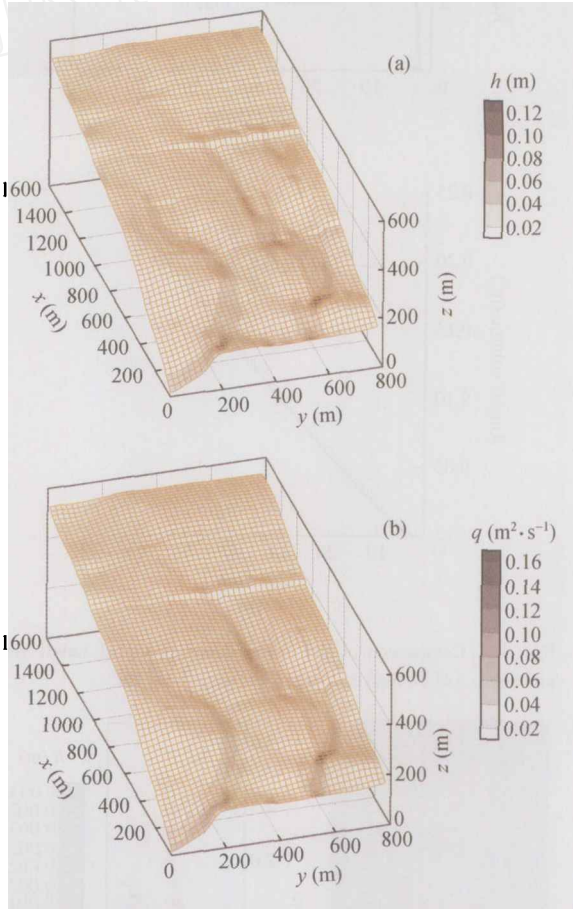

Fig. 7. Distributions of water depths and unit discharges of runoff on the Maoping slope. (a) Water depth of runoff; (b) unit discharge of runoff.

Fig. 9 shows the distributions of simulated velocity values and velocity vectors of runoff on the Maoping slope. The results clearly reveal the concentrated flow routes. Especially, the simulated velocity vectors reflect ideally the directions of runoff concentration, and exhibit the whole picture of surface runoff flow on the Maoping slope.

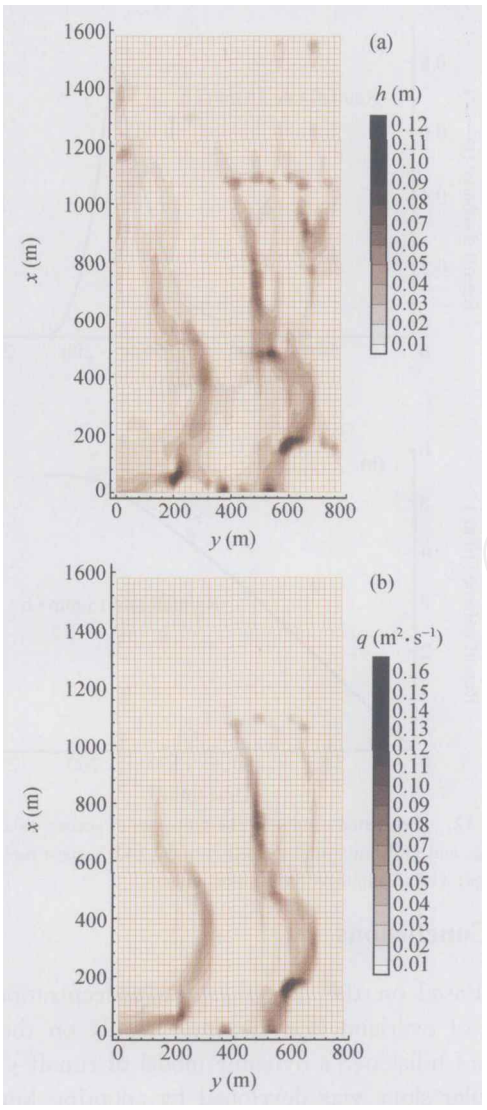

Fig. 8. Plane views of distributions of water depths and unit discharges of runoff on the Maoping slope. (a) Water depth of runoff; (b) unit discharge of runoff.

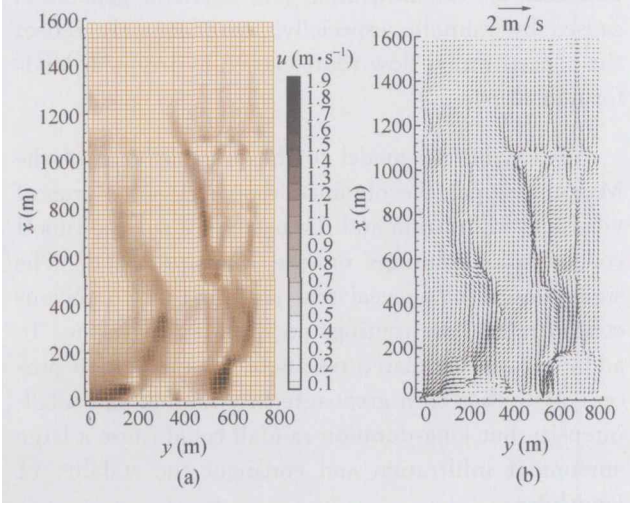

Fig. 9. Plane view of distribution of velocities of runoff on the Maoping slope. (a) Distribution of velocity values of surface runoff; (b) distribution of velocity vectors of surface runoff.

3.3.2 Processes of runoff yield and infiltration on the surface of the Maoping slope

Changing the rainfall condition, the processes of runoff yield and infiltration on the Maoping slope were simulated for four rainfall intensities of 30, 60, 90, and 120 mm/h with the same rainfall duration of 1 hour. The calculated values of runoff discharge and infiltration amount as functions of time for various rainfall intensities, respectively, are shown in Fig. 10 and Fig. 11. The simulated results show that both the total runoff and the total infiltration increase with the increasing rainfall intensity. A rainfall of one-hour duration may lead to the infiltration amount of 4×10^4 m^3, which shows that the infiltration caused by rainfall is fairly large. Besides intenerating soil and increasing pore pressure, infiltration water coming from rainfall could obviously increase the deadweight of slope body, which also casts bad impact on the stability of landslides. When there exist fractures on slopes, especially when the fractures are located in the surface flow route, rainfall water may lead much more infiltration into the slope body. Therefore, effective drainage measure is significant for the protection of landslide.

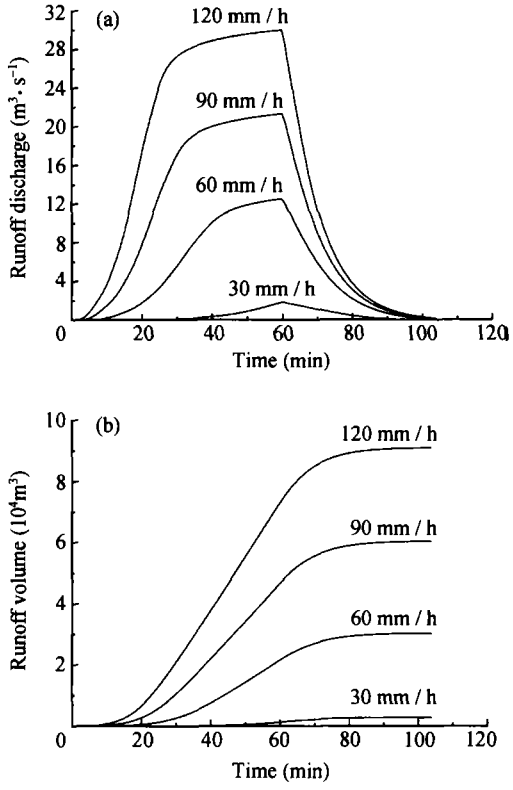

Fig. 10. Simulated results of runoff generation processes for different rainfall intensities. (a) Runoff discharge; (b) accumulated amount of surface runoff.

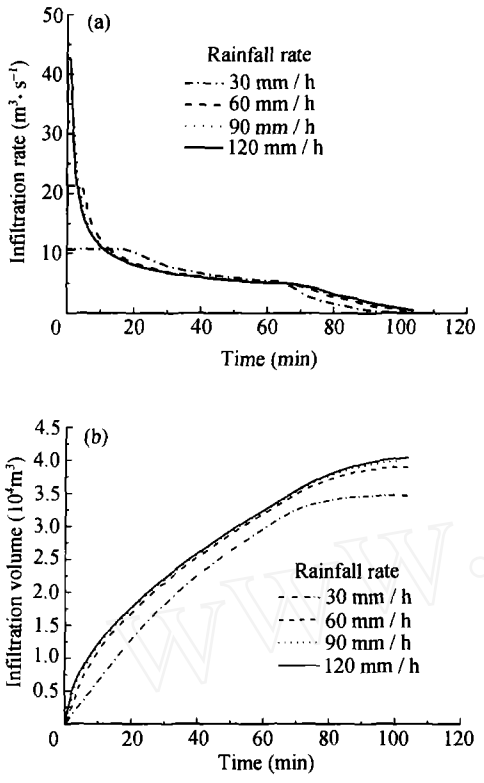

Fig. 11. Simulated results of the process of infiltration on surface soil for different rainfall intensities. (a) Infiltration rate for total slope; (b) accumulated infiltration amount for total slope.

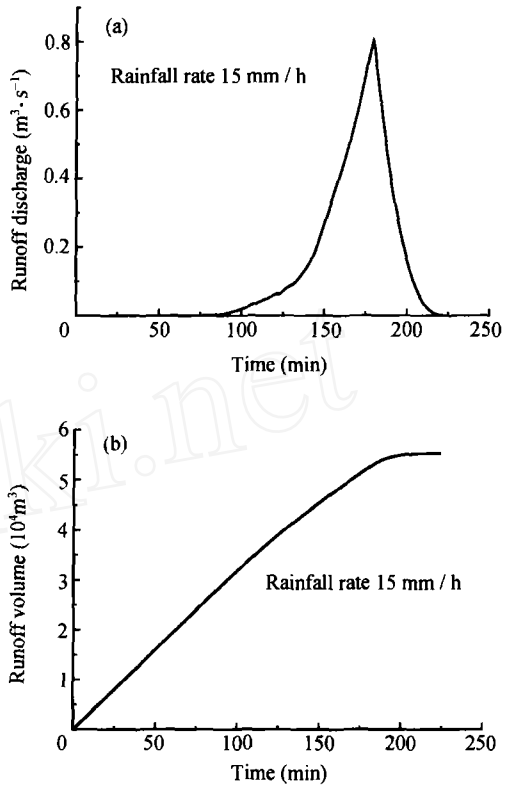

Fig. 12. Simulated results on the processes of surface runoff discharge and infiltration under small rainfall. (a) Surface runoff discharge; (b) accumulated infiltration amount.

For the small-intensity but long-duration rainfall, the process of surface runoff and infiltration was simulated for the rainfall at the intensity of 15 mm/hour for 3 hours. Fig. 12 shows the calculated results of the processes of runoff yield and infiltration, which indicates that when rainfall intensity is small the surface runoff is also small, but the infiltration amount will reach a rather great value. The simulated results demonstrate that the small-intensity but long-duration rainfall, likewise, can cause a large amount of infiltration and endanger the stability of landslide.

Table 1 compares the ratio of total infiltration amount to total rainfall under different rainfall intensities. The results show that the ratio of total infiltration amount to total rainfall increases with the decrease of rainfall intensity, which indicates that small rainfall could also lead to great rain infiltration. Moreover, the small-intensity, but long-duration rainfall may result in more infiltration, and is further adverse for the stability of landslide.

Table 1. The ratio of infiltration amount to total rainfall under different rainfall conditions

Rainfall intensity (mm/h)	15	30	60	90	120
Infiltration amount/total rainfall (%)	95.96	90.39	50.78	34.67	26.29

4 Conclusions

Based on the fact that the concentration flow route of overland flow depends mainly on the landform of hillslope, a dynamic model of runoff yield on irregular slope was developed by adopting kinematic wave theory and revised Green-Ampt infiltration formula. This model is able to reasonably simulate the processes of soil infiltration and overland generation caused by rainfall, especially, to adequately reflect the concentration flow route caused by irregular landform of slopes.

Applying the model to the practical case of the Maoping slope, we obtained the processes of runoff yield and infiltration and the pattern of surface runoff concentration routings on the Maoping slope. The simulation results reveal that there exist two obvious concentrated flow routings on the Maoping slope. In addition, the simulated results of the infiltration process show that both great-intensity rainfall and small-intensity but long-duration rainfall could cause a large amount of infiltration and endanger the stability of landslides.

As a matter of fact, the complex landform and

vegetation cover have some influences on the rainfall trapping and soil properties on the Maoping slope. Because of the lack of the spot observation, the present study did not account for these effects caused by landform and vegetation cover. Nevertheless, the results presented in this paper, especially the simulated results of the runoff concentration process and the pattern of concentrated flow route, could offer an important foundation for designing the surface drainage engineering on the Maoping Slope.

Acknowledgement The authors would like to thank Mr. Wei Zhiyan for his help in the data compilation and the part calculation.

References

1 Iverson R.M. Landslide triggering by rain infiltration. Water Resources Research, 2000, 36(7): 1897—1910.
2 Chen H. and Lee C. F. A dynamic model for rainfall-induced landslides on natural slopes. Geomorphology, 2003, 51: 269—288.
3 Hanenberg W.C. Observation and analysis of pore pressure fluctuations in a thin colluvium landslide complex near Cincinnati Ohio. Engineering Geology, 1991, 31: 159—184.
4 Angeli M.G., Pasuto A. and Silvano S. A critical review of landslide monitoring experiences. Engineering Geology, 2000, 55: 133—147.
5 Yao H.L., Zheng S.H., Li W.B. et al. Parametric study on the effect of rain infiltration on stability of unsaturated expansive soil slope. Journal of Rock Mechanics and Engineering (in Chinese), 2002, 21(7): 1034—1039.
6 Scoging H. Modeling overland-flow hydrology for dynamic hydraulics. In: Overland Flow (ed. Parsons A. J. and Abrahams A. D.), London: UCL Press, 1992, 89—103.
7 Govindaraju R. S., Kavvas M. L. and Tayfur G. A simplified model for two-dimensional overland flows. Advances in Water Resources, 1992, 15: 133—141.
8 Tayfur G. Modeling two-dimensional erosion process over infiltration surfaces. Journal of Hydrologic Engineering, 2001, 6(3): 259—262.
9 Michael B.A. and Refsgaard J.C. Distributed Hydrological Modeling. Netherland: Kluwer Academic Publishers, 1996.
10 Cao W.H., Qi W., Guo Q.C. et al. Distributed model for simulating runoff yield in small watershed. Journal of Hydraulic Engineering (in Chinese), 2003, 9: 48—56.
11 Li J.C., Liu Q.Q. and Zhou J.F. Environmental mechanics research in China. Advances in Applied Mechanics, 2003, 39: 217—306.
12 Liu Q. Q., Chen L., Li J.C. et al. Two-dimensional kinematic wave model for overland-flow. Journal of Hydrology, 2004, 291: 28—41.
13 Schmid B. H. On the overland modeling: can rainfall excess be treated as independent of flow depth? Journal of Hydrology, 1989, 107: 1—8.
14 Singh V. P. Kinematic Wave Modeling in Water Resources: Surface Water Hydrology. New York: John Wiley & Sons, 1996.
15 Mein R. G. and Larson C. L. Modeling infiltration during a steady rain. Water Resources Research, 1973, 9(2): 384—394.
16 Woolhiser D. A. and Ligget J.A. Unsteady, one dimensional flow over a plane—The rising hydrograph. Water Resources Res., 1967, 3(3): 753—771.
17 Chen L. and Liu Q.Q. On the equations of overland flow and one dimensional equations for open channel flows with lateral inflow. Mechanics in Engineering (in Chinese), 2001, 23(4): 21—24.
18 Liu Q. Q. and Singh V. P. Effect of micro-topography, slope length and gradient and vegetative cover on overland flow. Journal of Hydrologic Engineering, 2004, 9(5): 375—382.
19 Deng J.H., Ma S.S., Zhang B.J. et al. Preliminary investigation on the activation of Maoping landslide, Geheyan reservoir, Qingjiang river. Journal of Rock Mechanics and Engineering (in Chinese), 2003, 22(10): 1730—1737.